

Electronic Supplementary Information

Near Neutral Waterborne Cationic Polyurethane from CO₂-polyol, a Compatible Binder to Aqueous Conducting Polyaniline for Eco-friendly Anti-corrosion Purpose

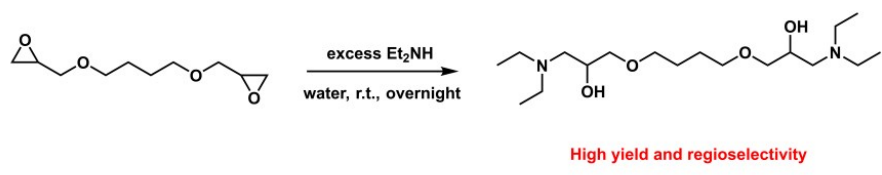
Chenyang Zou,^{a,b} Hongming Zhang,^a Lijun Qiao,^a Xianhong Wang^{*a,b} and Fosong Wang^{a,b}

^a Key Laboratory of Polymer Eco-materials, Changchun Institute of Applied Chemistry, Chinese Academy of Sciences, Changchun 130022, People's Republic of China.
Corresponding authors: E-mail: xhwang@ciac.ac.cn or hmzhang@ciac.ac.cn;

^b University of Science and Technology of China, Hefei, Anhui 230026, People's Republic of China

Contents

Synthesis and characterization of BDE	P2-P5
Synthetic protocols for all CPUDs	P6-P10
The calcultion equation of N ⁺ content	P11
GPC traces and ¹ H-NMR spectrum for all CPUDs	P12-P20
¹ H-NMR spectrum and GPC spectrum of CO ₂ -polyols	P21-P22
FT-IR spectrum for PPC-BDE-4	P23
Measurements on water absorption rate of different CPUDs films	P24
Thermal properties for various CPUD films	P25-P27
DSC curves for PPC-BDE-2/4/6	P28
SEM images of the fracture surface for PPC-BDE-4(0.8)	P29
Disperison compatibility investigations for composite coatings	P30



Scheme 1. Reaction of 1,4-butanediol diglycidyl ether with diethylamine in water.

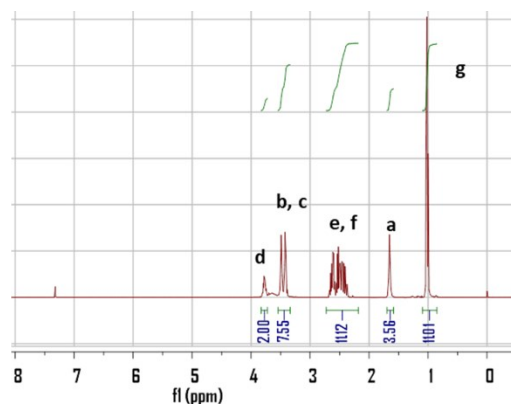
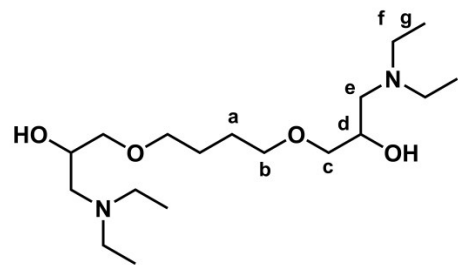


Fig. S1 The ^1H -NMR spectrum of BDE in CDCl_3 .

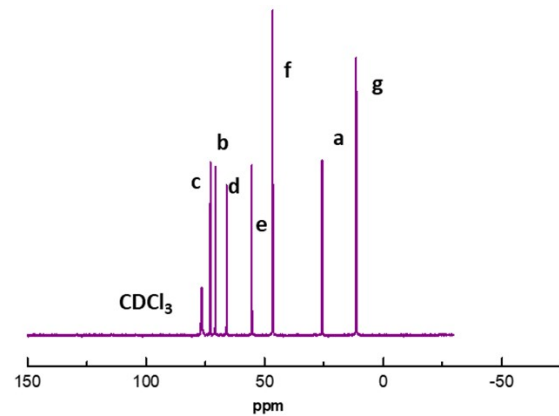


Fig. S2 The ^{13}C -NMR spectrum of BDE in CDCl_3 .

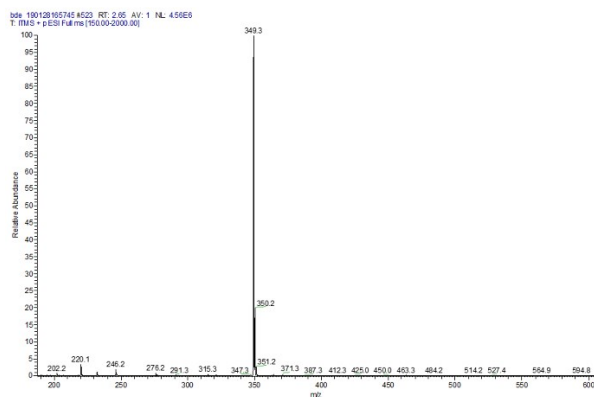


Fig. S3 The mass spectrometry of BDE in positive mode.

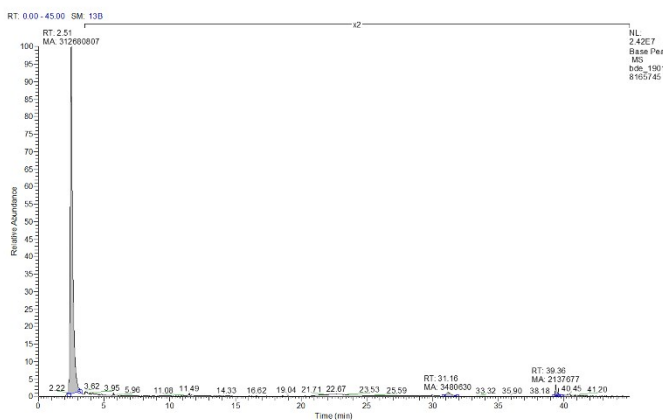


Fig. S4 The HPLC-MS was used to determine the purity for BDE, up to 98.3%.

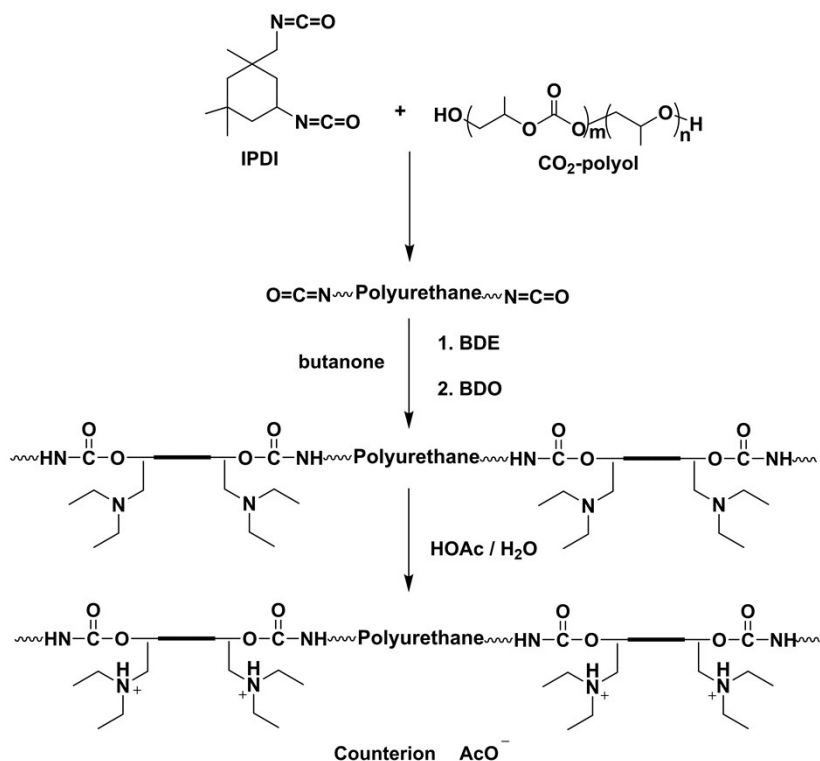


Fig. S5 Synthetic route to prepare CPUD using BDE as internal emulsifier with different contents of hydrophilic group and neutralization degree.

Synthesis of PPC-BDE-2

To a three-necked round bottom flask equipped with a mechanical stirrer and a condenser, 5.0 g of butanone, 20.70 g of PPC-diol (CU% of 56%) and 9.11 g of IPDI were added under N₂ protection, and then 0.08 g of DBTDL was added as catalyst, the reaction was carried out at 80 °C for 2 h. The reaction lasted another 6 h at 60 °C after 0.704 g of BDE was added in one portion, subsequently 2.66 g of BDO was added and the reaction was maintained at 60 °C for another 2 h, the endpoint of every step was monitored by FT-IR technique. To neutralize the tertiary amine, 0.24 g of HOAc was added to produce the quaternary ammonium salts (QAS), and water was added dropwise with vigorous stirring after 30 min. The butanone was removed under reduced pressure at 40°C to obtain PPC-BDE-2.

Synthesis of PPC-BDE-6

Synthesized using the same method as PPC-BDE-2.

26.85 g of PPC-diol; 11.814 g of IPDI; 2.68 g of BDE; 2.99 g of BDO; 0.924 g of HOAc

Synthesis of PPC-BDE-4/PPC-BDE-4(1)/PPC-BDE-4(0.8)

Synthesized using the same method as PPC-BDE-2.

38.10 g of PPC-diol; 16.76 g of IPDI; 2.55 g of BDE; 4.57 g of BDO

0.88 g of HOAc for PPC-BDE-4; 0.44 g of HOAc for PPC-BDE-4(1); 0.35 g of HOAc for PPC-BDE-4(0.8)

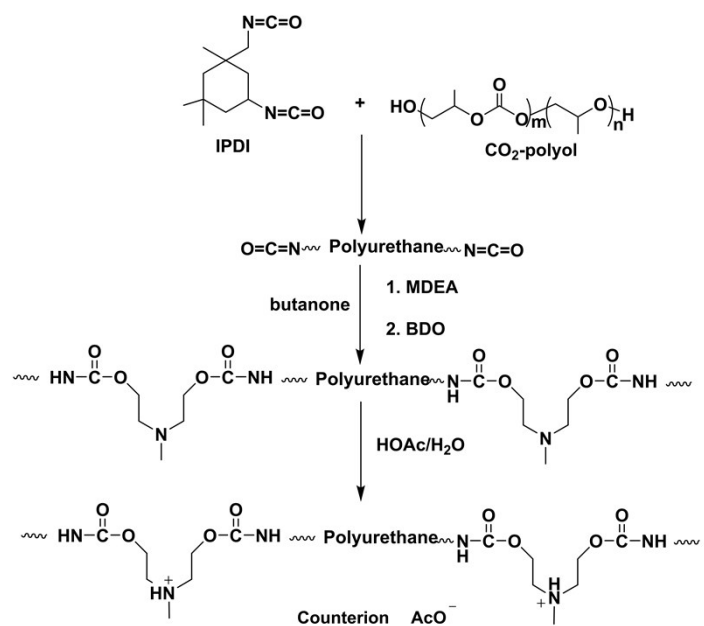


Fig. S6 Synthetic route to prepare PPC-MDEA-4.

Synthesis of PPC-MDEA-4

Synthesized using the same method as PPC-BDE-2.

37.18 g of PPC-diol; 16.36 g of IPDI; 2.424 g of MDEA; 3.27 g of BDO; 1.22 g of HOAc

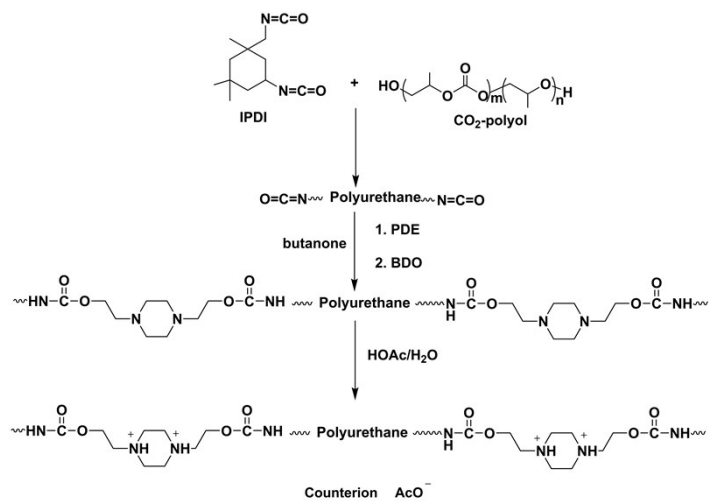


Fig. S7 Synthetic route to prepare PPC-PDE-5.

Synthesis of PPC-PDE-5

Synthesized using the same method as PPC-BDE-2.

15.89 g of PPC-diol; 6.99 g of IPDI; 1.30 g of PDE; 1.51 g of BDO; 0.89 g of HOAc

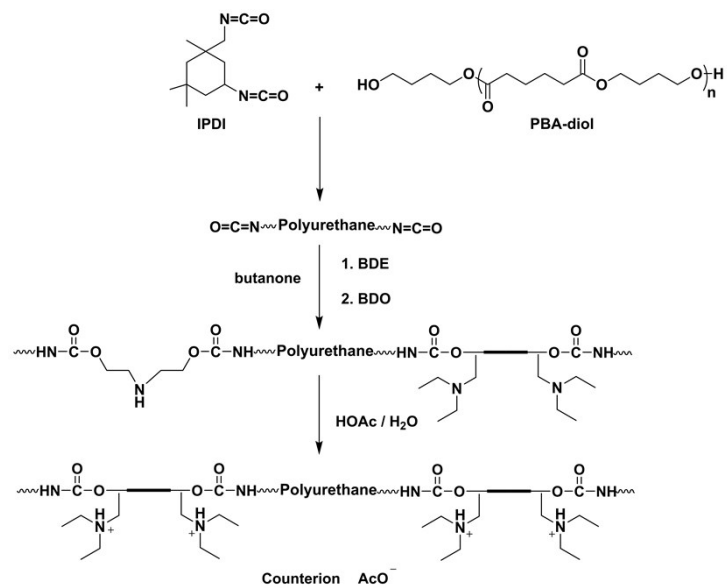


Fig. S8 Synthetic route to prepare PBA-BDE-4.

Synthesis of PBA-BDE-4

Synthesized using the same method as PPC-BDE-2.

31.79 g of PBA-diol; 13.99 g of IPDI; 2.25 g of PDE; 3.657 g of BDO; 0.776 g of HOAc

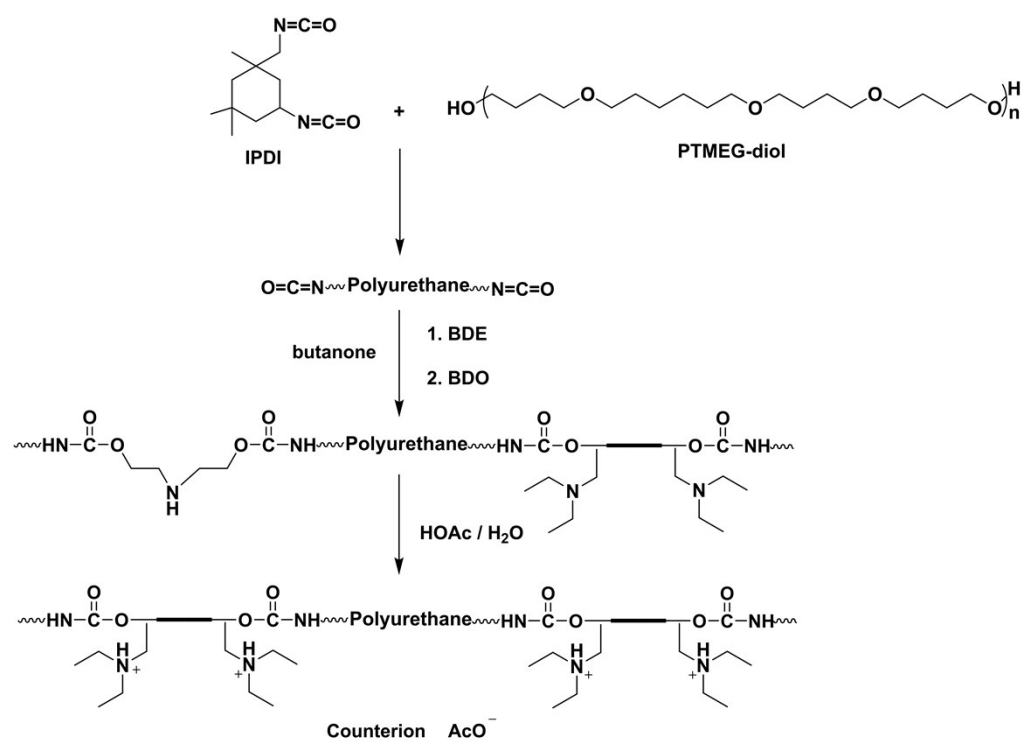


Fig. S9 Synthetic route to prepare PTMEG-BDE-4.

Synthesis of PTMEG-BDE-4

Synthesized using the same method as PPC-BDE-2.

18.65 g of PBA-diol; 8.206 g of IPDI; 1.25 g of PDE; 2.163 g of BDO; 0.43 g of HOAc

$$\text{Content (N⁺, %)} = \frac{m(CE)}{m(\text{polyol}) + m(IPDI) + m(BDO) + m(CE)} \times \frac{M(N)}{M(CE)} \times \frac{n(HOAc)}{n}$$

$m(CE)$, $m(\text{polyol})$, $m(IPDI)$ and $m(BDO)$ are their respective mass, so the first term represents the content of hydrophilic group; $M(N)$ means the sum of relative atomic mass of nitrogen in a molecule and $M(CE)$ is the relative molecular mass of chain extender, so the second term represents the mass fraction of nitrogen atoms; $n(HOAc)$ refers to the actual molar amount of HOAc used in the preparation process and n is the theoretical molar amount of HOAc required under the assumption of 100% neutralization, therefore the third term represents the degree of neutralization.

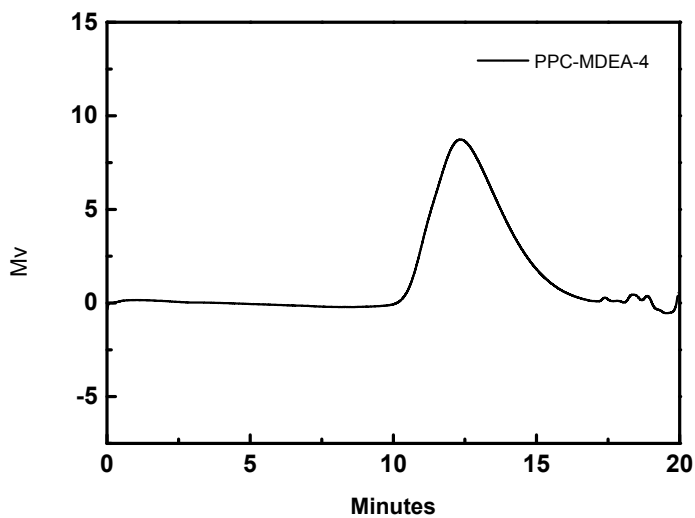


Fig. S10 GPC traces of PPC-MDEA-4.

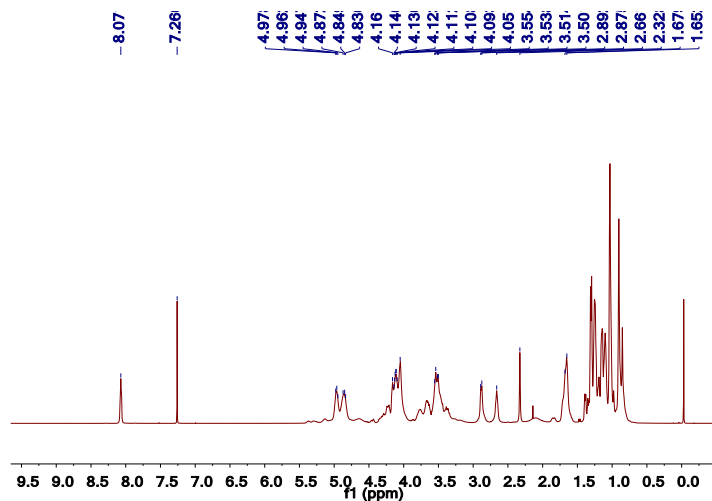


Fig. S11 ¹H-NMR spectrum of PPC-MDEA-4.

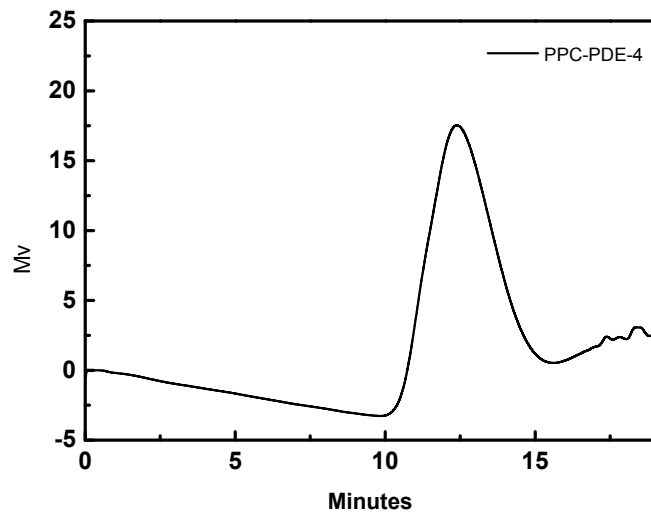


Fig. S12 GPC traces of PPC-PDE-5.

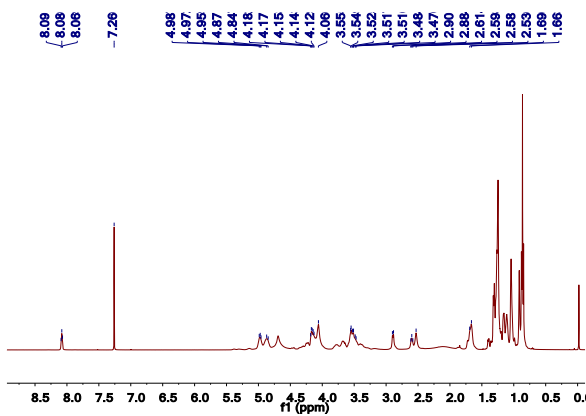


Fig. S13 ¹H-NMR spectrum of PPC-PDE-5.

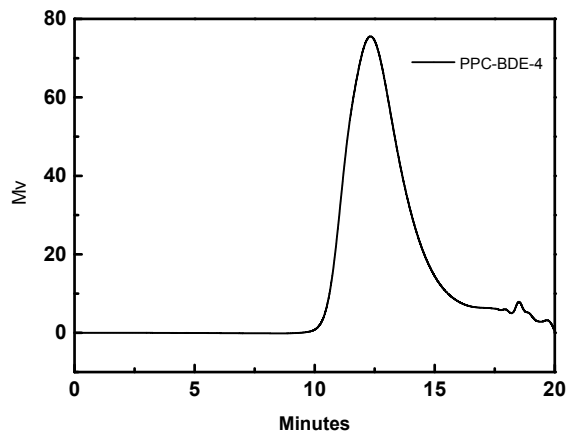


Fig. S14 GPC traces of PPC-BDE-4.

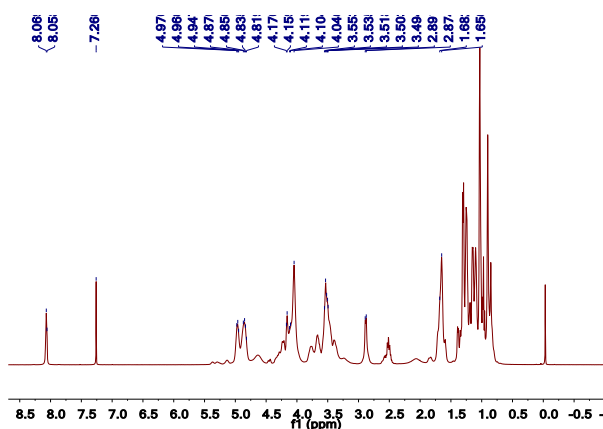


Fig. S15 ¹H-NMR spectrum of PPC-BDE-4.

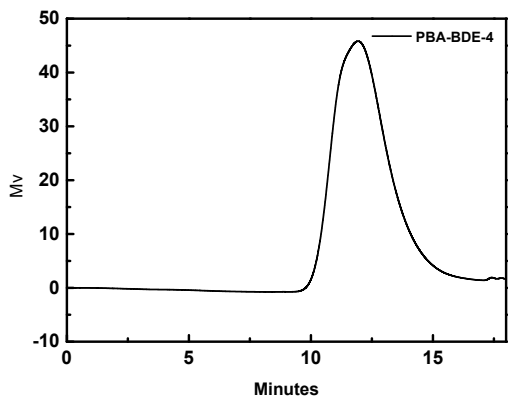


Fig. S16 GPC traces of PBA-BDE-4.

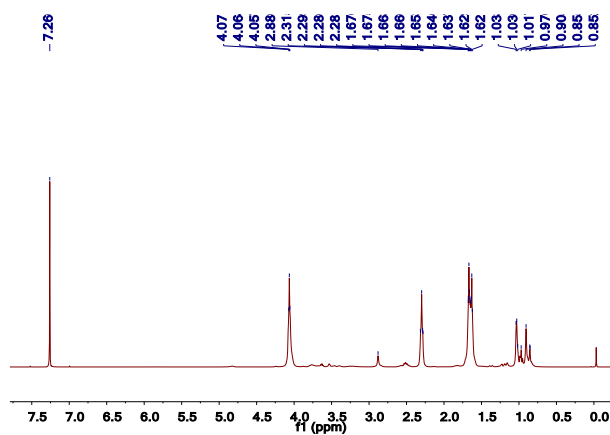


Fig. S17 ¹H-NMR spectrum of PBA-BDE-4.

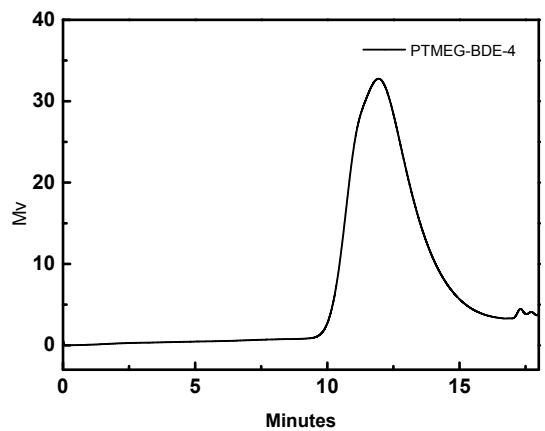


Fig. S18 GPC traces of PTMEG-BDE-4.

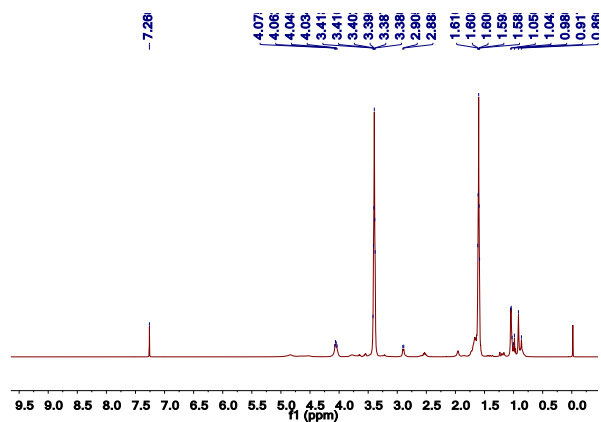


Fig. S19 ¹H-NMR spectrum of PTMEG-BDE-4.

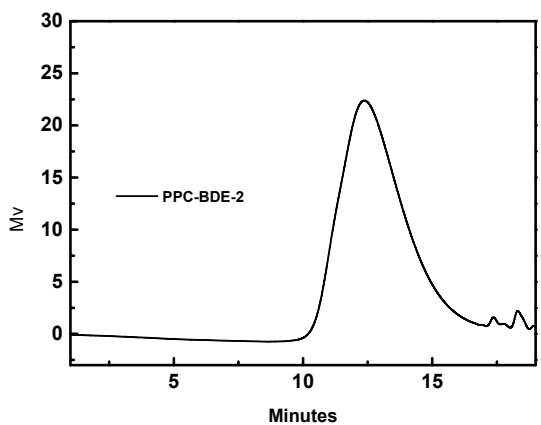


Fig. S20 GPC traces of PPC-BDE-2.

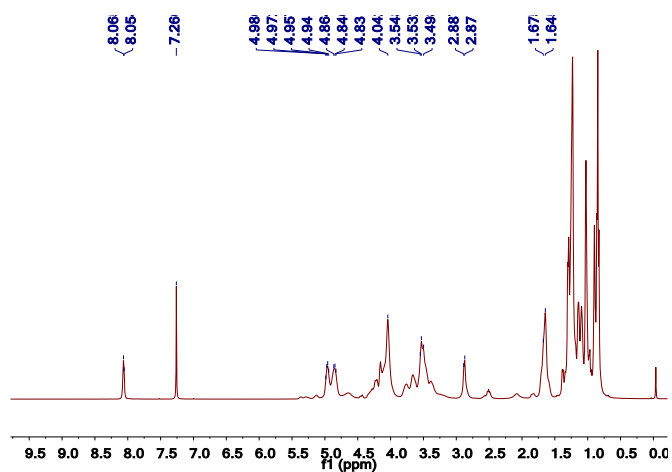


Fig. S21 ¹H-NMR spectrum of PPC-BDE-2.

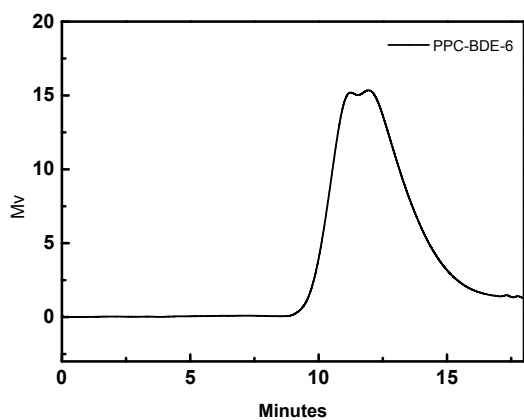


Fig. S22 GPC traces of PPC-BDE-6.

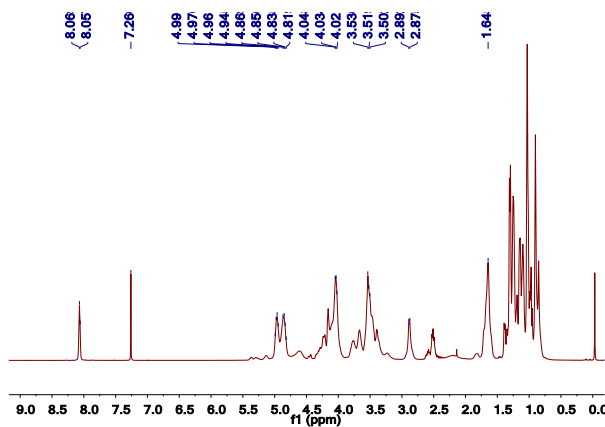


Fig. S23 ¹H-NMR spectrum of PPC-BDE-6.

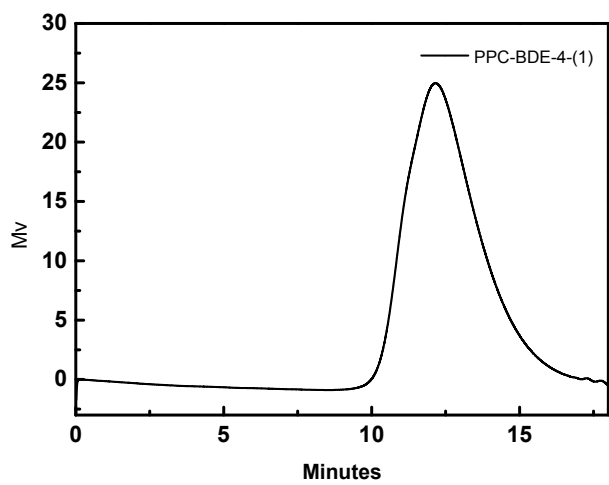


Fig. S24 GPC traces of PPC-BDE-4(1).

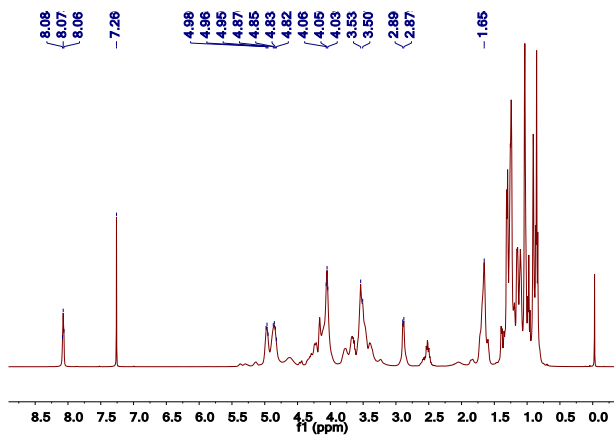


Fig. S25 ¹H-NMR spectrum of PPC-BDE-4(1).

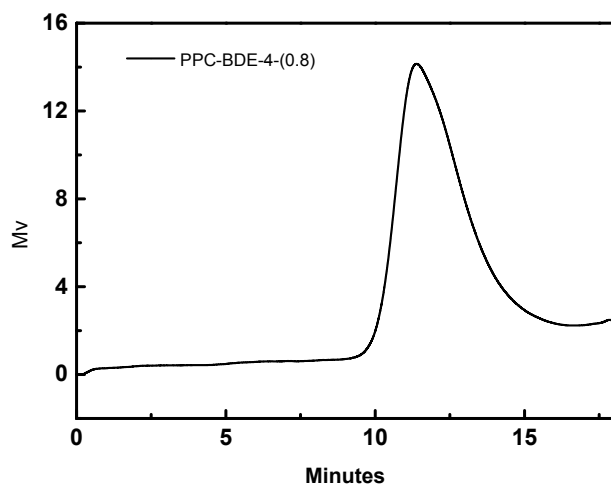


Fig. S26 GPC traces of PPC-BDE-4(0.8).

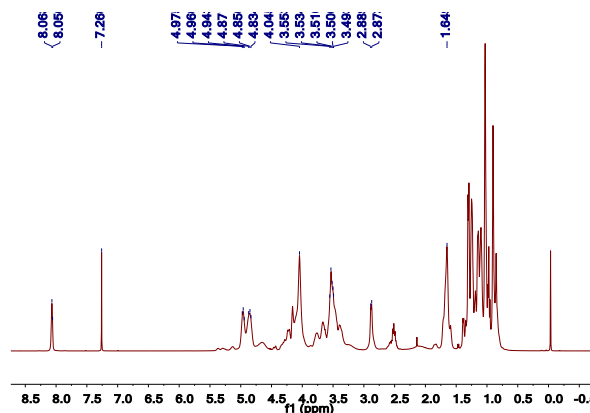


Fig. S27 ¹H-NMR spectrum of PPC-BDE-4(0.8).

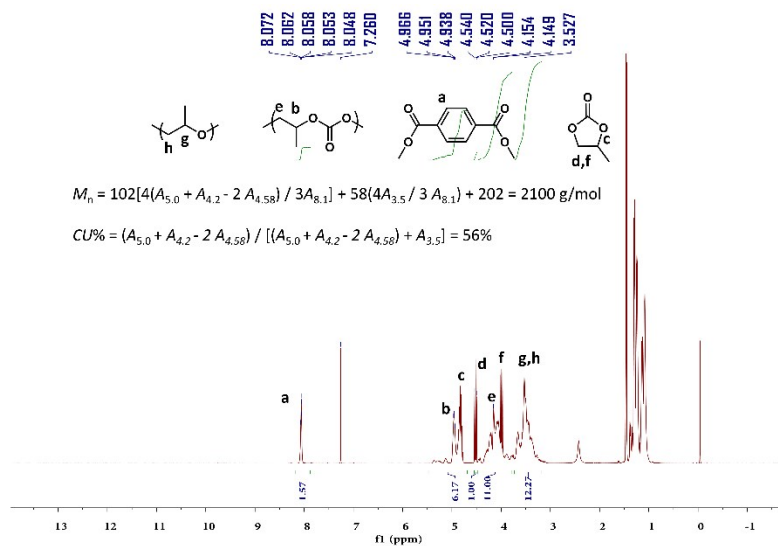


Fig. S28 The ^1H -NMR spectrum of CO₂-polyols in CDCl₃.

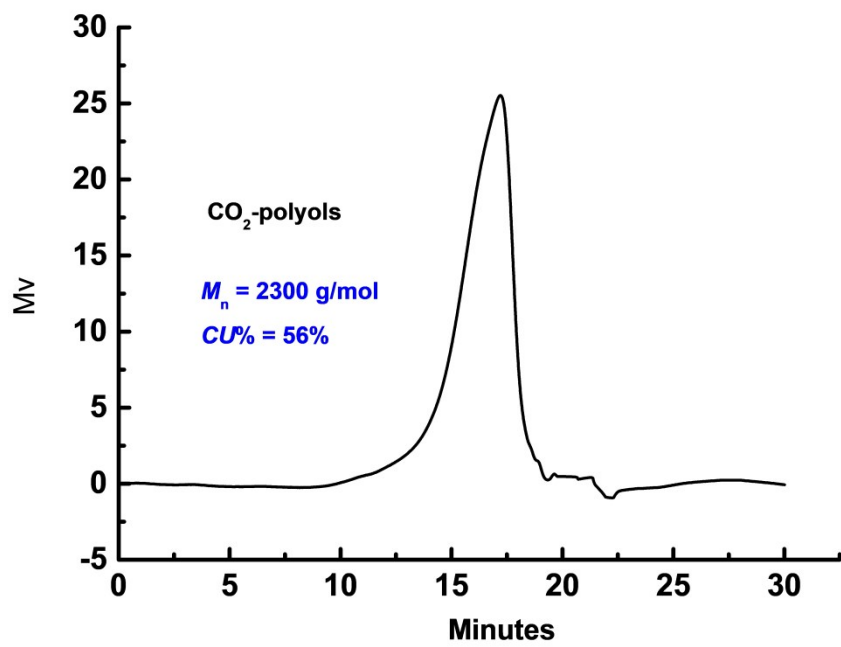


Fig. S29 The GPC spectrum of CO₂-polyols with CU% of 56%.

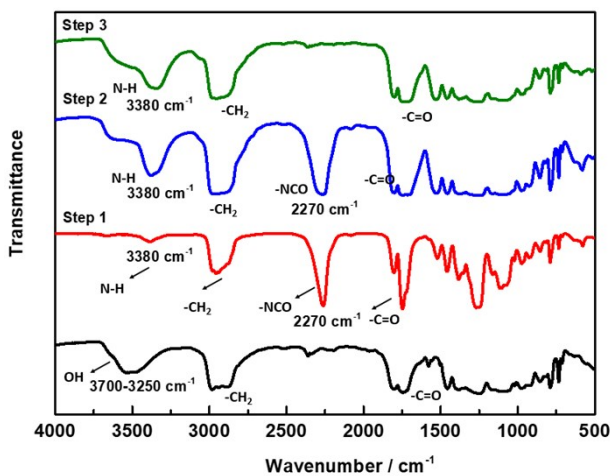


Fig. S30 Monitoring the synthesis process of PPC-BDE-4 utilizing the FT-IR technology. Step 1 showed the spectrum after 2h when PPC (56%) and IPDI were mixed. Step 2 and Step 3 represent the spectrum after 4h and 2h when BDE and BDO were added to the system, respectively.

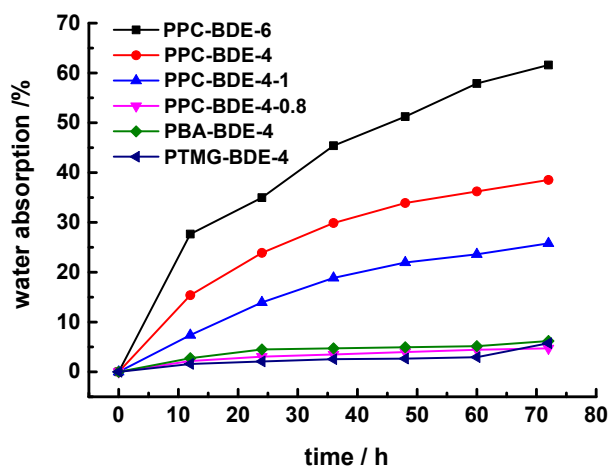


Fig. S31 Dependence of water absorption rate of different CPUDs films on immersion time in deionized water at room temperature.

Table S1. Thermal properties for PPC-MDEA-4, PPC-PDE-5, PPC-BDE-2, PPC-BDE-4 and PPC-BDE-6.

Designation	T_5 [°C]	T_{50} [°C]	T_{\max} [°C]
PPC-MDEA-4	209.1	302.3	305.8
PPC-PDE-5	182.6	285.9	308.1
PPC-BDE-2	216.3	307.8	319.4
PPC-BDE-4	211.7	306.6	307.8
PPC-BDE-6	205.9	303.7	314.8

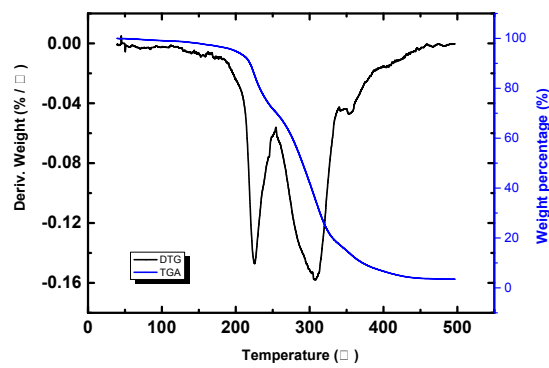


Fig. S32 TGA and DTG curves for PPC-MDEA-4.

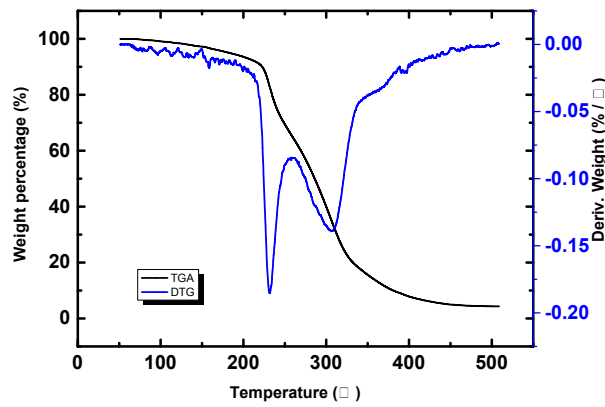


Fig. S33 TGA and DTG curves for PPC-PDE-5.

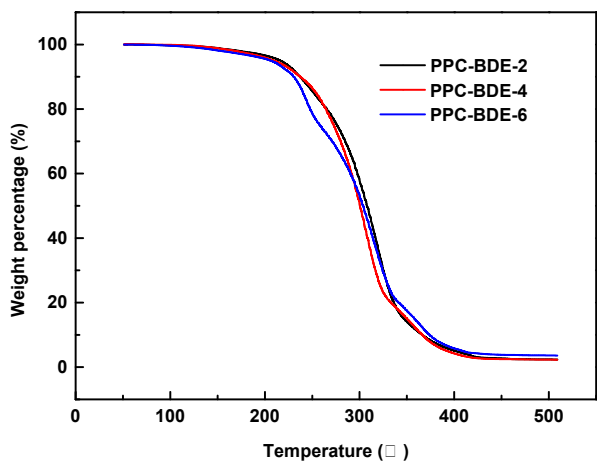


Fig. S34 TGA curves for PPC-BDE-2/ PPC-BDE-4/ PPC-BDE-6.

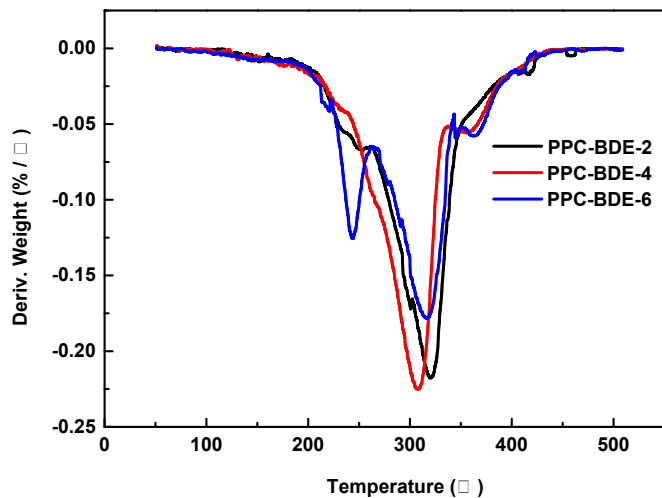


Fig. S35 DTG curves for PPC-BDE-2/ PPC-BDE-4/ PPC-BDE-6.

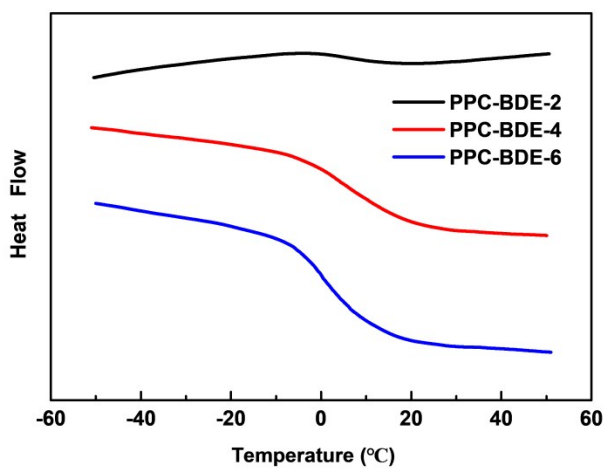


Fig. S36 The DSC curves for PPC-BDE-2 ($T_g = 5.16\text{ }^{\circ}\text{C}$), PPC-BDE-4 ($T_g = 3.27\text{ }^{\circ}\text{C}$) and PPC-BDE-6 ($T_g = -0.06\text{ }^{\circ}\text{C}$).

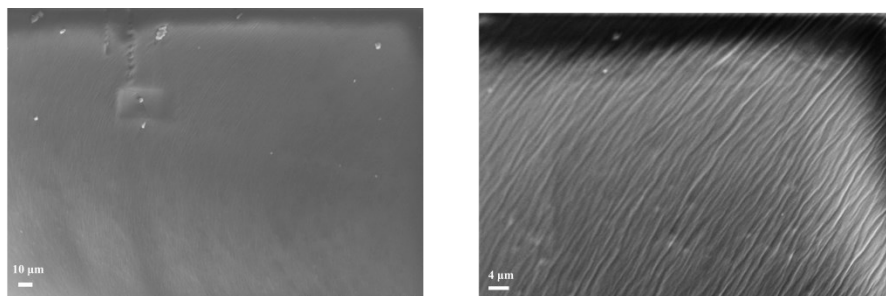


Fig. S37 SEM images of fracture surface for PPC-BDE-4(0.8).

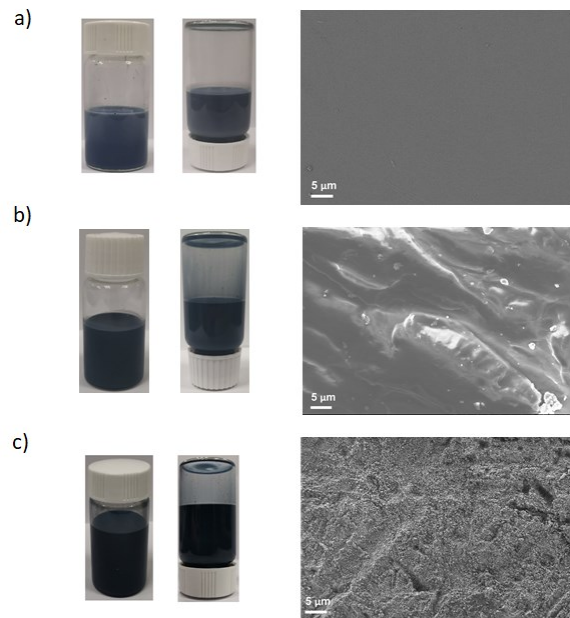


Fig. S38 Images of the composite dispersion in a transparent vial after standing for 20 days (left) and the cross section SEM image of fracture surface (right) for 0.5 wt% cPANI/CPUD (a), 2.0 wt% cPANI/CPUD (b) and 3.0 wt% cPANI/CPUD (c).